

ADAPTIVE MECHANISMS FOR RECONFIGURABLE MACHINES BASED ON DEFORMABLE CAM

Dr. MARCO SILVESTRI

Department of Engineering and Architecture, University of Parma, Parma, Italy &

Department of Innovative Technologies, SUPSI, Manno, Switzerland

ABSTRACT

This paper presents an innovative solution to make configurable an automatic machine based on a mechanical cam through the adoption of a cam with a flexible profile, controlled in a certain number of precision points by means of motors driving a recirculating ball screw. The dynamic effect of the followers on the flexible profile requires an iterative process to determine the kinematic performance of the system and the constructive aspects have been considered in detail, designing an original mechanism with positive guidance for the realization of the followers. The results obtained demonstrate the feasibility of the solution and the performances comply with the design requirements.

KEYWORDS: Adaptive Mechanism, Deformable Cam, Finite Element Analysis & Reconfigurable Machine

Received: May 18, 2019; **Accepted:** Jun 08, 2019; **Published:** Jul 06, 2019; **Paper Id.:** IJMPERDAUG201960

INTRODUCTION

Modern packaging machines are often based on a rotating table architecture, generally having considerable size, which allows to obtain high production rates and requires a precise synchronization of the machine part movements [1][2][3]. In this scenario, the use of mechanical cams for the vertical movement of the devices positioned along the external circumference is often preferred to electric motor driven systems both because more competitive cost and for undisputed reliability in all operating conditions[4][5]. These important advantages, however, have as counterpart the need to proceed with format changeover operations whenever a modification to the motion law described by the cam itself is required [6][7].

There is therefore the need to identify new solutions that guarantee the best tradeoff between reliability requirements[8][9] at high speed and the possibility of adapting the machine recipe with an automated, fast and repeatable procedure[10][11]. For this purpose, an original solution is proposed here, which consists in the adoption of a deformable mechanical element which performs the function of a cam and which can be adapted by means of the deformation imposed by some electric actuators controlled in position by the machine PLC [12] [13].

The study takes into consideration the kinematic characteristics of the obtained law of motion and the main constructive challenges related to the adoption of the proposed solution [14]. To illustrate it, a specific application example has been investigated using a finite element analysis and an original constructive solution has been proposed for the realization of the follower element.

The machine consists of a main rotating table where the production process is implemented, equipped with two smaller ones that act as input and an output transfer system.

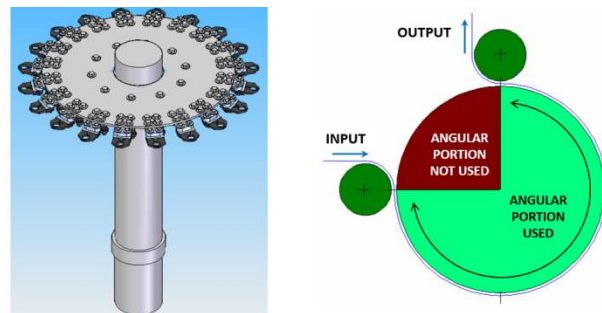


Figure 1: Example of Machine Rotating Table

Deformance Cam

To make configurable a cam follower mechanism, various approached have been proposed [15][16][17]. In the present study, the concept solution consists in adopting a flexible cam means a cam composed of an elastic material and to deform it by actuating a certain number of position-controlled motors to obtain a sufficiently accurate approximation of the requested law of motion [18] [19]. Such an approach has been inspired by the well-known drawing tool called *spline* which consists in a thin wood or metal strip used to interpolate a given set of fixed points: the deformable strip acts as a translating cam, coupled with a translating follower used to control the vertical movement of the tools, as shown in Figure 2.

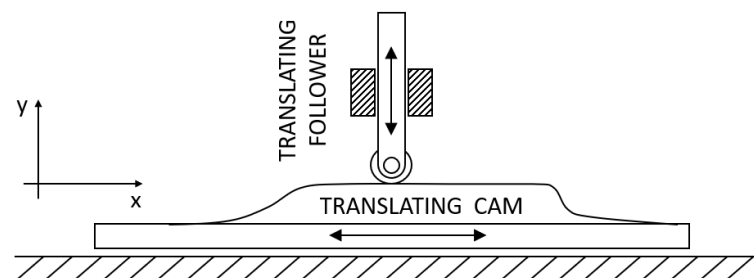


Figure 2: Translating Cam – Translating Follower Mode of Input/Output Motion

The mechanical behavior of this deformable element has been analyzed with the aid of the finite element method (FEM) software ABAQUS®, the use of which is widespread in the mechanical industry. Such approach to structural analysis is based on the discretization of the starting continuous domain in a discrete domain (mesh) through the use of primitives (finite elements) of simple form (triangle and quadrilateral for 2D domains, hexahedron and tetrahedron for 3D domains).

Any structure can be analyzed through FEM, through the following main steps: 1. define the geometric model (size and shape of the structure); 2. define the primitive to be used to discretise the structure; 3. define the dimension of the elements; 4. define the boundary conditions (applied loads, applied constraints, material, etc.).

Concerning the supports, it should be observed that when the cam is deformed to obtain the desired lift, it must necessarily shorten itself, so it must be supported by two roller connections at its ends, as shown in Figure 3. A third constraint is given by another roller support to prevent the translation along z and to impose the desired deformation along the y axis.

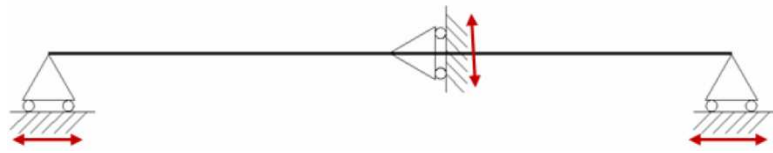


Figure 3: Cam Roller Connections

In fact the number of points where the deformation must be imposed is one of the most critical aspect in this study, as illustrated in the next paragraphs; its value has been determined as a consequence of the kinematic analysis performed. Being the cam section rectangular, generating its mesh results simple: the face is divided with elements at the same distance to obtain elements of square shape. Likewise, in the longitudinal direction the surface is divided into squares, obtaining 3D cubic elements. The overall result is shown in Figure 4, where arrows indicate the areas of greatest deformation.

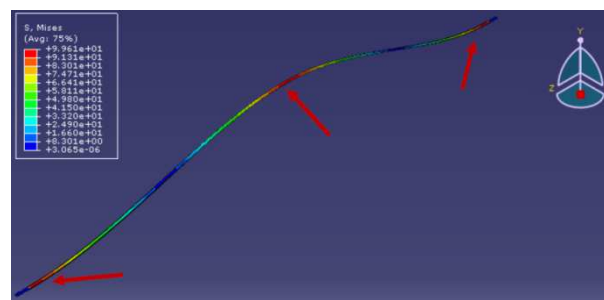


Figure 4: Visualization of the Deformations Calculation

Moreover, partitions are created in the areas of greatest stress, which are the areas near the cam connections and which require a thickening of the mesh to achieve the convergence of the analysis, as shown in Figure 5.

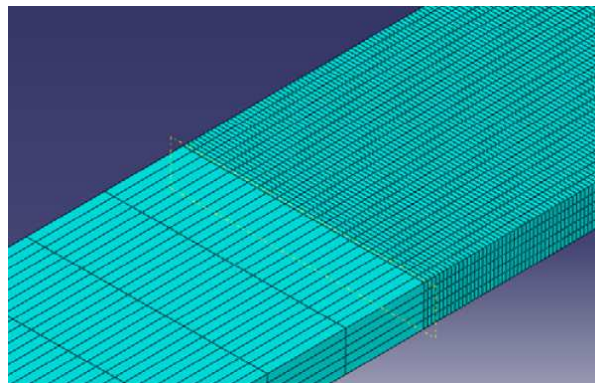


Figure 5: Difference in Discretization between the Connection Areas and Other Parts of the Cam

To optimize the tradeoff between the discretization level and the calculation time, an analysis has been performed, verifying that the result converges for element size less than or equal to 0.5 mm^3 , as illustrated in Figure 6.

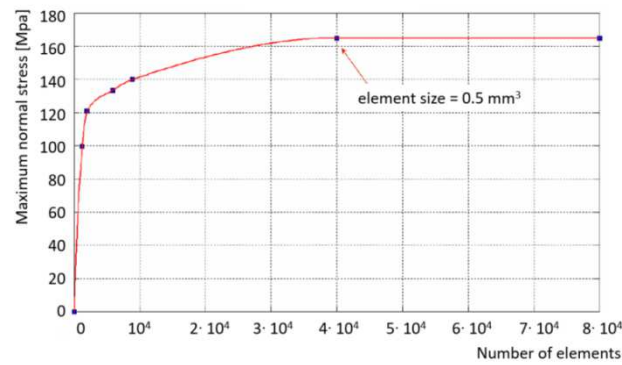


Figure 6: Convergence of 20x5mm Rectangular Plate Mesh

Moreover, it is necessary to verify how stress varies on increasing the width of the cam section to find the optimal tradeoff between its value and the possibility to obtain a greater coupling area for the follower wheels. Figure 7 shows the almost linear relationship calculated between cam width and maximum stress.

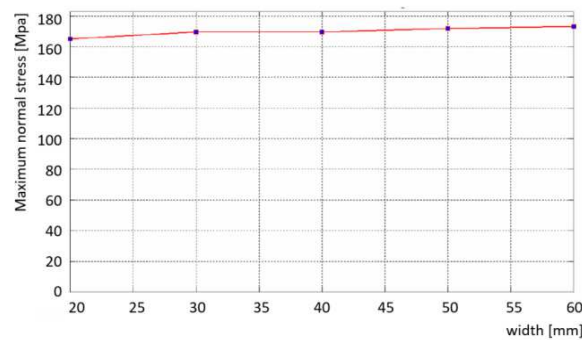


Figure 7: Stress on Varying the Cam width

With regard to the cam-follower coupling, it is also necessary to leave the passage to the lower wheel on the cam lower face through an appropriate extension of the width of the cam in the support areas. The stress generated by these section variations has been verified, as shown in Figure 8.

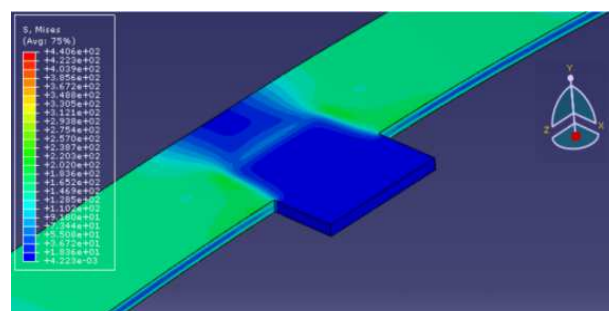


Figure 8: Finite Element Analysis of the Constraint Support

Finally, to limit stress on the motor screw, it is necessary allow a relative rotation between cam and rods through a revolute pair, as illustrated in Figure 9.

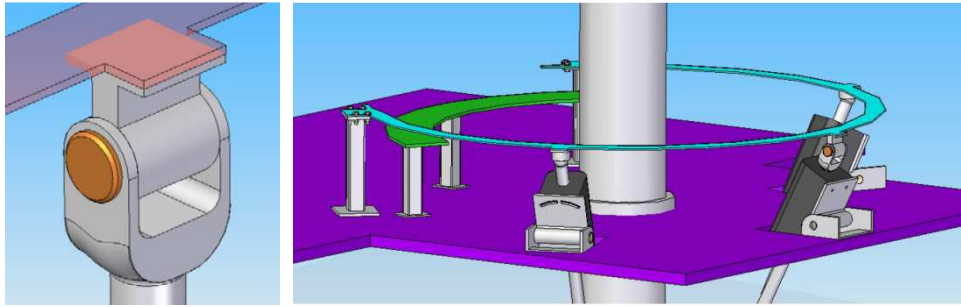


Figure 9: Revolute Pair Constraint on the Positioning Rods

FOLLOWER

The design of the follower system started from the consideration that a positive mechanical constraint had to be preferred, because of its capability to always guarantee, together with the elements contact, to limit the oscillations that may arise due to the possible cam twisting generated together with the cam vertical deformation. Usually this design solution is based on having two rollers, separated by a fixed distance, which act as the constraint, but in this case the lower part of the cam is only in part available and a possible radial deformation must be compensated too. The designed solution is shown in Figure 10, where the red wheel is the main wheel that supports the weight of the mechanism and transmits the motion, while the yellow one is the lower wheel that creates the positive constraint, and which have reduced dimensions to roll on a narrower track.

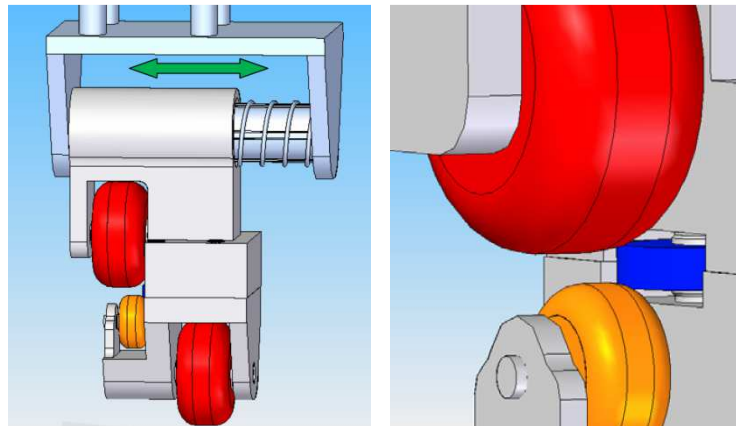


Figure 10: Positive Constraint (Vertical) and Spring Constraint (Radial)

Moreover, the blue wheel, combined with the action of a spring, maintains the follower always in contact with the guide in a radial direction with a spring constraint mounted on a grooved profile which acts as a prismatic guide and prevent the relative rotation between the lower and the higher part of the follower. Finally, the lower red wheel is necessary when the follower passes from the mobile part of the cam to the fixed one. In the transition section from one guide to the other, the two cams will overlap, allowing a smooth passage. In this area both wheels are engaged, as clarified in Figure 11, where the fixed cam is drawn in green and the deformable one is drawn in blue.

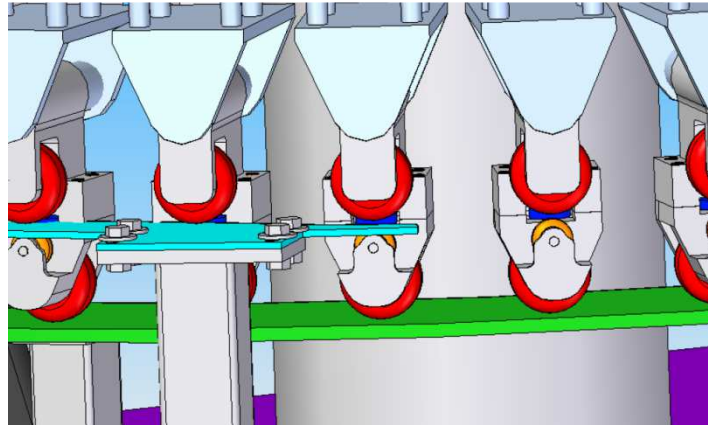


Figure 11: Change of Driving from Flexible to Fixed

Kinematic Analysis

The kinematic study of the system is non-trivial because the cam final deformation also depends on the stress that the follower exerts on it, which in turn depends on the acceleration. Therefore, it is necessary to proceed iteratively, by first studying the law of motion determined by the cam deformation and the dynamic effect of the follower.

To analyze the system kinematic behavior, it can be considered, carried out on a plane, as the linear cam-follower system shown in Figure 2, where the absolute velocity of the follower can be broken down into two components: the frame velocity along y and the relative one along x:

$$\vec{v}_a = \vec{v}_r + \vec{v}_f \quad (1)$$

Where the frame velocity is:

$$v_f = \omega \cdot R \quad (2)$$

Being ω the angular speed of the table and R its radius.

Regarding the relative speed, it is of course:

$$v_r = \frac{dy}{dt} \quad (3)$$

Which can be also be written as:

$$v_r = \frac{dy}{d\theta} \cdot \frac{d\theta}{dt} = v_y(\theta) \cdot \omega \quad (4)$$

And the other term:

The velocity $v_y(\theta)$ has been calculated by as the derivative of the lift diagram with respect to the angle θ , writing a Matlab® program to apply the method of the central derivatives. Figures 12, 13 and 14 show the obtained results, which can be interpreted considering the lift curve close to the combination of two cubic polynomial curves, the velocity one as the combination of two nearly parabolic curves and finally the acceleration as the combination of two almost straight-line segments.

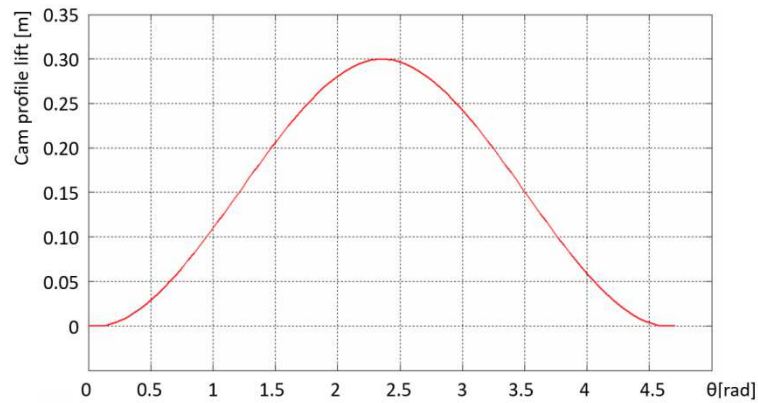


Figure 12: Resulting Cam Profile

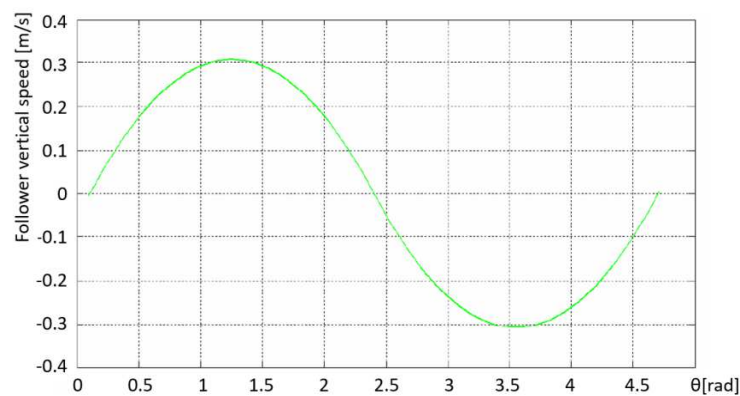


Figure 13: Resulting Follower Speed

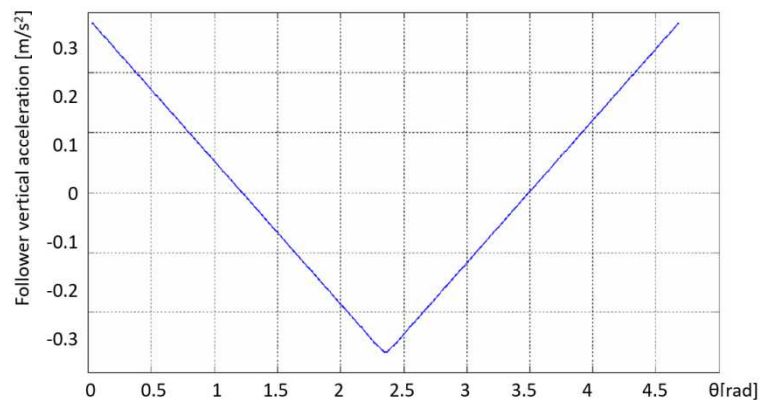


Figure 14: Resulting Follower Acceleration

Dynamic Analysis

To calculate the force exerted on the cam, the system can be schematized as in Figure 15, where φ is the angle of friction, α is the cam pressure angle, and F_p the weight. Wheel friction and revolute pair friction are neglected.

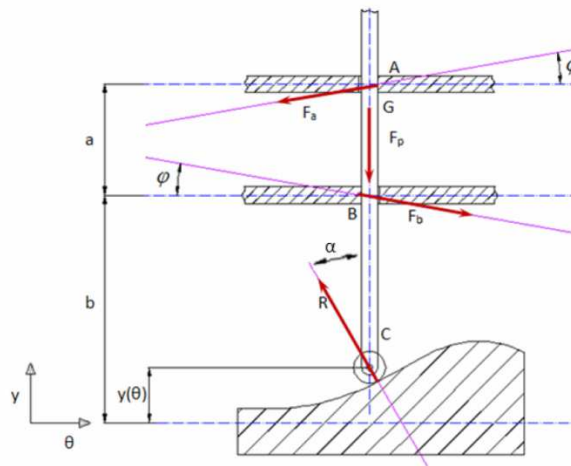


Figure 15: Balance of Forces Applied on the Follower

The pressure angle α is equal to:

$$\alpha = \arctan \frac{dy}{d\theta} \quad (5)$$

It varies on the rotating angle θ as shown in Figure 16.

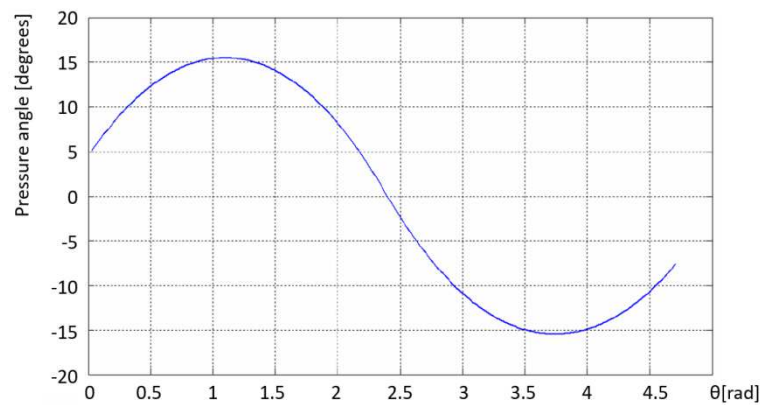


Figure 16: Pressure Angle

The cardinal equations of dynamics can be written as:

$$m \cdot \vec{a}_G = \vec{F}_a + \vec{F}_b + \vec{F}_p + \vec{R} \quad (6)$$

$$\dot{K}_c = \vec{F}_b \times \vec{BC} + \vec{F}_a \times \vec{AC} \quad (7)$$

where: m is the mass of the mobile system, \vec{a}_G is the acceleration of point G, \dot{K}_c is the derivative of the angular momentum, which is equal to:

$$K_c = \vec{CG} \times m \cdot \vec{v}_a = \vec{CG} \times m \cdot (\vec{v}_r + \vec{v}_f) \quad (8)$$

Where \vec{v}_a is the absolute speed, equal to the sum of the relative speed \vec{v}_r and the frame speed \vec{v}_f . The vector product between the relative speed and \vec{CG} is null since they have the same direction, then:

$$K_c = \vec{CG} \times m \cdot \vec{v}_t \quad (9)$$

Replacing \vec{v}_t it can be written as:

$$K_c = CG \cdot m \cdot \omega \cdot R \quad (10)$$

Being the derivative of constant terms null, it results:

$$\dot{K}_c = 0 \quad (11)$$

Then the vector resolution of equation (7) gives:

$$\begin{cases} m \cdot a_t = -F_a \cdot \cos \phi + F_b \cdot \cos \phi - R \cdot \sin \alpha \\ m \cdot a_r = -F_a \cdot \sin \phi - F_b \cdot \sin \phi - R \cdot \cos \alpha \\ 0 = F_a \cdot \cos \phi \cdot AC_y - F_a \cdot \sin \phi \cdot AC_x - F_b \cdot \cos \phi \cdot BC_y + F_b \cdot \sin \phi \cdot BC_x \end{cases} \quad (12)$$

Where:

$$BC_y = b - y(\vartheta) \quad (13)$$

$$AC_y = BC_y + a \quad (14)$$

By solving the system and using a Matlab® program, graphs of the reaction forces on varying θ have been obtained. They are shown in Figure 17 and 18 and it can be observed that there is no detachment between the wheel and the guide, as R_x is always positive.

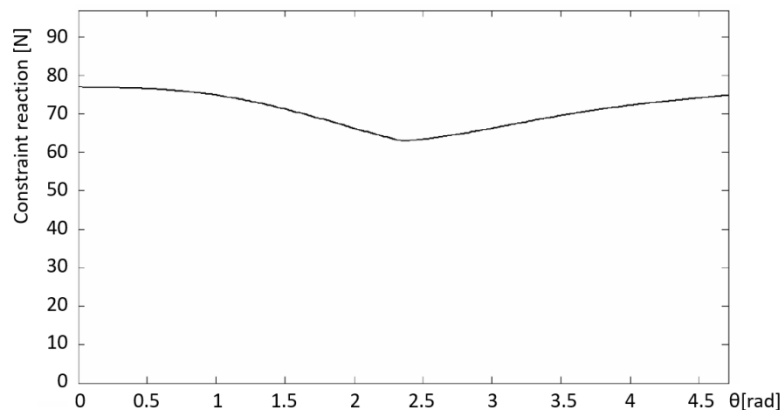


Figure 17: Constraint Reaction R

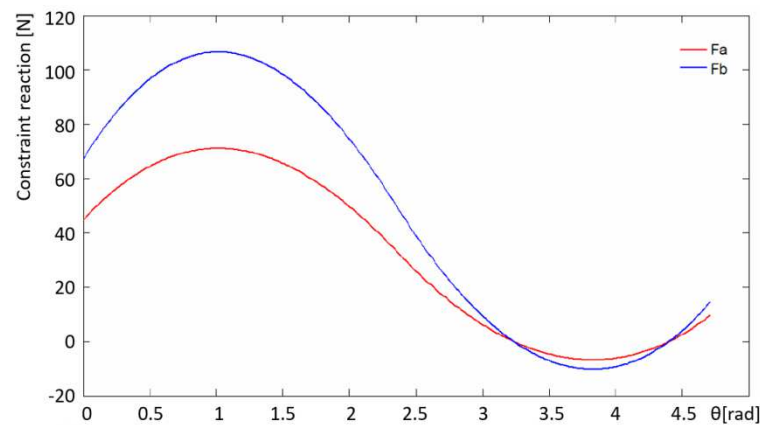


Figure 18: Constraint Reaction Fa and Fb

Finally, the application of the force exerted by the followers on the cam determine a new deformation calculation, shown in Figure 19, which presents a peak stress equal to 1680 MPa, which is obviously not acceptable, and too large deformation on the intermediate points indicated by the red arrows in the figure. To maintain a deformation corresponding to the motion law calculated, it is therefore necessary to set two other supports. In Figure 20 it can be seen how the maximum stress is considerably diminished and the deformations remains close to the desired shape. In the next paragraph a quantitative analysis of these results is performed.

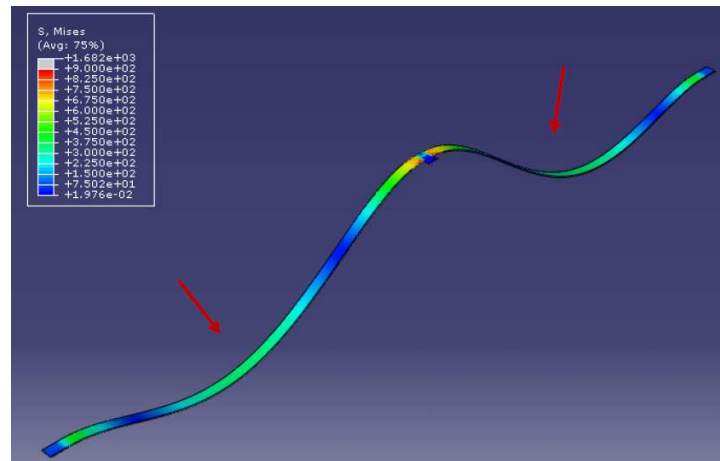


Figure 19: Deformation Calculation with the Follower Forces and One Support

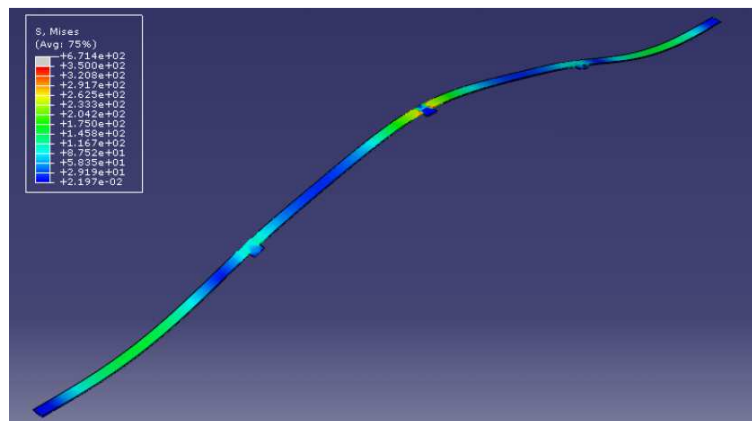


Figure 20: Deformation Calculation with the Follower Forces and Three Supports

RESULTS AND CONCLUSIONS

At the end of the iterative procedure described above, the obtained results are used to create a final model of the ring-shaped cam with three supports to impose a specific position, shown in Figure 21.

To proceed with an accurate analysis of the characteristics obtained in terms of kinematic parameters, is calculated a spline curve that approximates the calculated deformation by means of 12 control points. The curve obtained, shown in Figure 22, has a maximum error of 0.6%, as it can be seen in Figure 2. The corresponding velocity and acceleration graphs are shown in Figure 24 and 25. Overall, the results obtained comply with the objectives set at the beginning of the research and demonstrate the practical reliability of the proposed method.

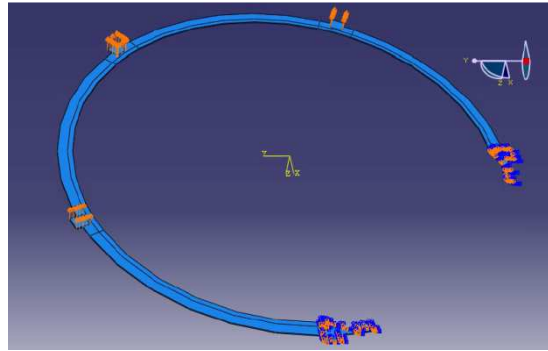


Figure 21: Final Cam Model

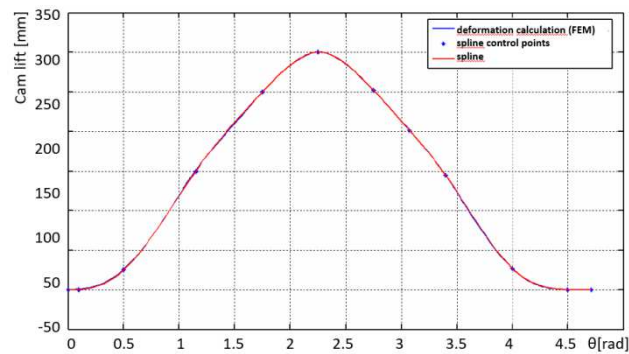


Figure 22: Final Spline Interpolation of the Cam

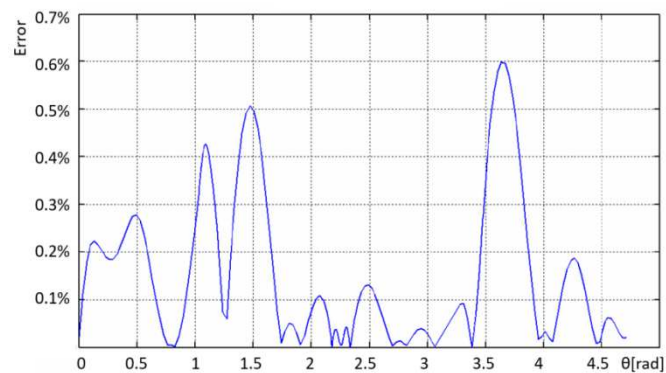


Figure 23: Difference between the Deformation Calculation and the Spline Interpolation

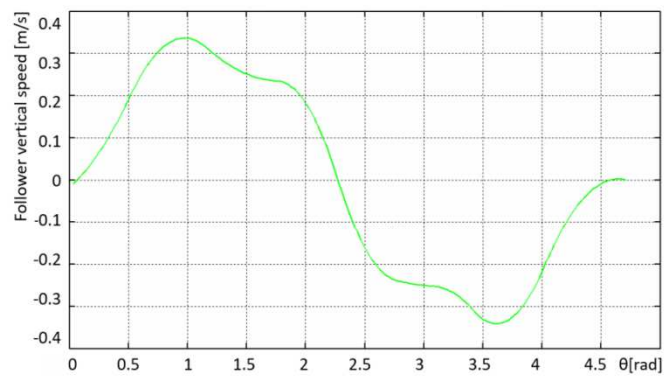


Figure 24: Final Vertical Speed

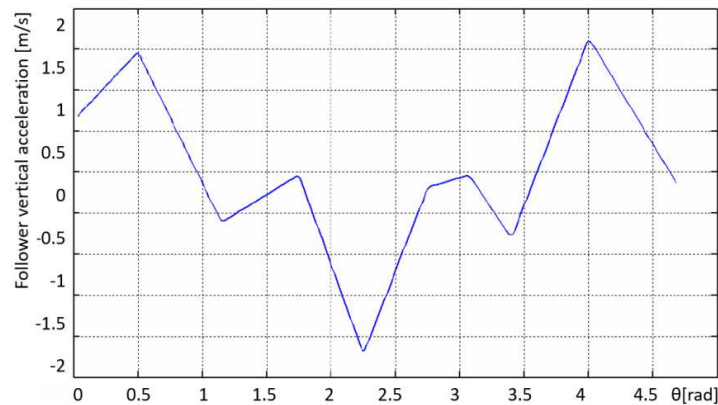


Figure 25: Final Acceleration

ACKNOWLEDGEMENTS

This work was made possible, thanks to the contribution provided by Eng. Daniel Mian in drawing the mechanical design and executing the finite element analysis.

REFERENCES

1. Ettlie, J.E., Reifeis, S.A., "Integrating Design and Manufacturing to Deploy Advanced Manufacturing Technology", *Inform Journal of Applied Analytics*, vol. 17-6, 1987, pp. 1-97
2. Avventuroso, G., Foresti, R., et. Al., "Production paradigms for additive manufacturing systems: A simulation-based analysis", 2017 ICE/ITMC, Madeira Island, Portugal, 2017, pp. 973-981. doi: 10.1109/ICE.2017.8279987
3. Giberti, H. and Pagani, A.: Flexibility oriented design of a horizontal wrapping machine, *Mech. Sci.*, 6, 109-118, <https://doi.org/10.5194/ms-6-109-2015>, 2015.
4. Rui-Ming Fang, Yi-Feng Lin, ZhangJie, "Conjugate cam design method of swing grippers mechanism on printing press", 2010 International Conference on Educational and Information Technology, 17-19 Sept. 2010, DOI: 10.1109/ICEIT.2010.5608346
5. Bayati I., Belloli M., Bernini L., et. al., "Scale model technology for floating offshore wind turbines", *IET Renewable Power Generation*, Volume 11, Issue 9, 12 July 2017, p. 1120 – 1126, DOI: 10.1049/iet-rpg.2016.0956
6. Giberti, H., Sbaglia, L., Silvestri, M., "Mechatronic Design for an Extrusion-Based Additive Manufacturing Machine". *Machines* 2017, 5, 29. doi:10.3390/machines5040029
7. Sbaglia, L., Giberti, H., et al., "The Cyber-Physical Systems within the industry 4.0 framework", *Advances in Italian Mechanism Science – Mechanisms and Machine Science* Volume 68, 2019, Pages 415-423, Springer Netherlands, DOI: 10.1007/978-3-030-03320-0_45
8. Ohnishi K., Shibata M., et Al., "Motion control for advanced mechatronics", *IEEE/ASME Transactions on Mechatronics*, vol. 1-1, 1996, pp. 56 – 6, DOI: 10.1109/3516.491410
9. Silvestri, M., Confalonieri, M., Ferrario, A., "Piezoelectric Actuators for Micro Positioning Stages in Automated Machines: Experimental Characterization of Open Loop Implementations", *FME Transactions* (2017) 45, 331-338, doi:10.5937/fmet1703331S
10. Giberti, H., Cinquemani, S., Legnani, G., "Effects of transmission mechanical characteristics on the choice of a motor-reducer", *Mechatronics* 2010, 20, 604–610

11. Hellmann, C.S., "Adjustable cam mechanism", Patent S2888837A
12. Bush, C.C., "Flexible cams", Patent US3680406A
13. Tarello, W., "Adjustable cam assembly", Patent US3792627A
14. Ying-min Han, Ning-ning Guo, et Al., "On Lateral Positioning Accuracy of the Die-Cutting Machine", *Electrical Engineering and Automation*, pp. 1083-1094, 2017, https://doi.org/10.1142/9789813220362_0128
15. Jian Hu, Yuangang Wang, et Al., "High-accuracy robust adaptive motion control of a torque-controlled motor servo system with friction compensation based on neural network", *Proceedings of the Institution of Mechanical Engineers, Part C: Journal of Mechanical Engineering Science*, Vol 233, Issue 7, 2019

